ELSEVIER

Biophysical Chemistry 91 (2001) 191–208

Biophysical Chemistry

www.elsevier.nl/locate/bpc

A fluorescence-based assay for transcription using a novel fluorescent GTP analogue

Srin Sastry*

Laboratory of Molecular Genetics, Box 174, The Rockefeller University, 1230 York Avenue, New York, NY 10021, USA

Received 15 February 2001; received in revised form 20 April 2001; accepted 26 April 2001

Abstract

A new fluorescent analogue of GTP (Cm-GTP) was synthesized, which contained a coumarin fluorophore attached to the gamma phosphorus. This compound was tested in transcription assays using T7 RNA polymerase as a model system. The fluorescent nucleotide was incorporated specifically at the 5′ end of nascent RNA synthesized in two different modes of transcription initiation. In the first mode, with only Cm-GTP (+GTP), reiterative slippage synthesis occurred and poly rG ladders of up to 14 nucleotides were synthesized. In the second mode, with Cm-GTP (+GTP) + ATP + CTP, abortive transcripts of up to seven or eight nucleotides were synthesized. The fluorescence properties of the two types of RNA were studied in detail. There was greater reduction in fluorescence intensity in G-ladders than in abortive transcripts. Steady-state anisotropy and anisotropy decay indicated that the fluorophore motion was constrained in G-ladder RNAs as compared to abortive RNAs. Quenching experiments by using extraneous quenchers showed that the excited state of fluorophore at the 5′ end of G-ladder RNA was less efficiently quenched as compared to the free fluorophore. These studies suggested that the fluorescent GTP analogue sensed the structural features that distinguished G-ladder RNAs from abortive RNAs. The results suggested that G-ladder RNAs adapt unusual conformations such as G-quartets. Thus, the new fluorescent probe can be useful for structural studies on RNA.

Keywords: Transcription; Nucleotide analogue; Fluorescence; Fluorescent probes; T7 RNA polymerase; RNA conformation; G-quartets

Abbreviations: Bp, base pairs; Cm, 7-amino-4-methyl coumarin; NTP, nucleoside triphosphate; PPi, pyrophosphate; T7 RNAP, bacteriophage T7 RNA polymerase; RNAP, RNA polymerase(s)

* Present address: 18255 73rd Avenue NE, Apartment C-104, Kenmore, WA 98028, USA. Tel.: +1-425-481-4866; fax: +1-425-481-4866.

E-mail address: sastrys2000@yahoo.com (S. Sastry).

0301-4622/01/$ - see front matter
PII: S0301-4622(01)00169-7

1. Introduction

Fluorescence is a versatile and highly sensitive technique for studying macromolecular interactions in biology. Fluorescence has the distinct advantage of being a non-invasive and non-disruptive technique that can be used to probe RNA and DNA structures and their interactions with proteins (numerous examples are given in refs. [1,2]). An example of a fundamental biological process that has received many applications of the fluorescence technique is transcription (e.g. [3–6]). In these studies, typically a ribonucleotide-conjugated fluorophore is incorporated into RNA and changes in the fluorescence properties (e.g. intensity, lifetime, anisotropy etc.) of the probe are measured in response to known changes in fluorophore environment. Quantitative analyses of the changes in spectral properties of the fluorophore are interpreted in terms of structure and interactions of the fluorophore-labeled RNA. A number of nucleotide analogues with fluorescent groups have been synthesized. However, a majority has the fluorescent group attached to the nucleobase itself or have fluorescent nucleobase mimics (e.g. ε-ATP [7,8], isoxanthopterin, a guanine analogue [9], 2-amino purine [10,11]). A potential drawback of modifying a nucleobase is that this could interfere with normal base pairing in nucleic acids or change the efficiency of utilization of the modified nucleotide by enzymes such as RNA and DNA polymerases. Problems could also arise if the modified nucleic acids were to fold to form specific conformations.

Here, I will report the synthesis of a new fluorescent GTP analogue that has a coumarin fluorophore attached to the γ-phosphate (Cm-GTP). I will demonstrate that this analogue is utilized by an RNA polymerase as efficiently as its natural counterpart. Furthermore, Cm-GTP's ability to sense conformational changes in RNA and its potential usefulness in studies of nucleic acid structure are demonstrated.

I chose transcription by T7 RNA polymerase as a test case for Cm-GTP because this prokaryotic RNA polymerase displays two types of transcription initiation that result in radically different RNA products: abortive RNAs; and slippage RNAs [12]. Slippage synthesis (also called stuttering) occurs with only GTP. Abortive synthesis, on the other hand, occurs in the presence of all four NTPs. Both modes of transcription initiation occur on native T7 RNA polymerase promoter. Slippage synthesis results in a monotonous poly-*r*G RNA of up to 14 nts, whereas abortive transcription results in up to 7–10 nts of RNA containing at least three of the four nucleotides. Thus, we have a good example in which two different species of RNA are made by the same enzyme. It is a well-known fact that poly-G containing nucleic acids form a large family of unusual structures collectively called G-quartets (reviewed in refs. [13,14]). Thus, it is almost axiomatic to suppose that poly-G ladders may display unusual conformations compared to abortive transcripts. I wished to test if the fluorescent Cm-GTP analogue could react differently to differences in RNA conformations between poly-G RNA (slippage reaction) and mixed sequence RNA (abortive reaction). The results indicate that the new fluorescent Cm-GTP analogue can be potentially used to distinguish unusual conformations in RNA and to possibly study RNA-protein interactions in the future.

2. Materials and methods

T7 RNAP was prepared employing published procedures [15,16]. GTP and 7-amino-4-methylcoumarin (Cm) and other chemicals were purchased from Sigma-Aldrich.

2.1. Synthesis of Cm-GTP

The synthesis was carried out in a similar manner as described before with some changes [17,18]. Twenty-five milligrams of GTP was dissolved in 1 ml of 125 mM 2-(*N*-morpholino)-ethanesulfonic acid buffer (pH 5.2) followed by the addition of 477 mg of 1-cyclohexyl-3,2-(morpholinoethyl) carbodiimide metho-*p*-toluenesulfonate (coupling agent). Two hundred milligrams of benzyltributylammonium chloride (phase transfer catalyst) was then added and the mixture was fully dissolved by

gentle rotation at room temperature (25°C) for 2.5 h. One hundred and eighty-five milligrams of Cm in 2 ml of dimethylformamide was added and the mixture was stirred for 4 h at room temperature. Portions of this solution were either subjected to analysis by TLC or were fractionated by using diethylaminoethyl sepharose (Pharmacia) followed by anion exchange HPLC. Cm-GTP ($\sim 20\%$ final yield) was eluted with a linear gradient of 0–0.5 M triethylammonium acetate or triethylammonium bicarbonate buffer (pH 7). The fluorescence quantum yield of Cm-GTP was determined relative to quinine sulfate in 0.1 N sulfuric acid as a reference standard ($E_x = 330$ nm and $E_m = 440$ nm, $\Phi_F = 0.51$) [19]. Cm-GTP ($\varepsilon_{342} = \sim 6000\ M^{-1}\ cm^{-1}$, $\Phi_F = 0.005$) was identified

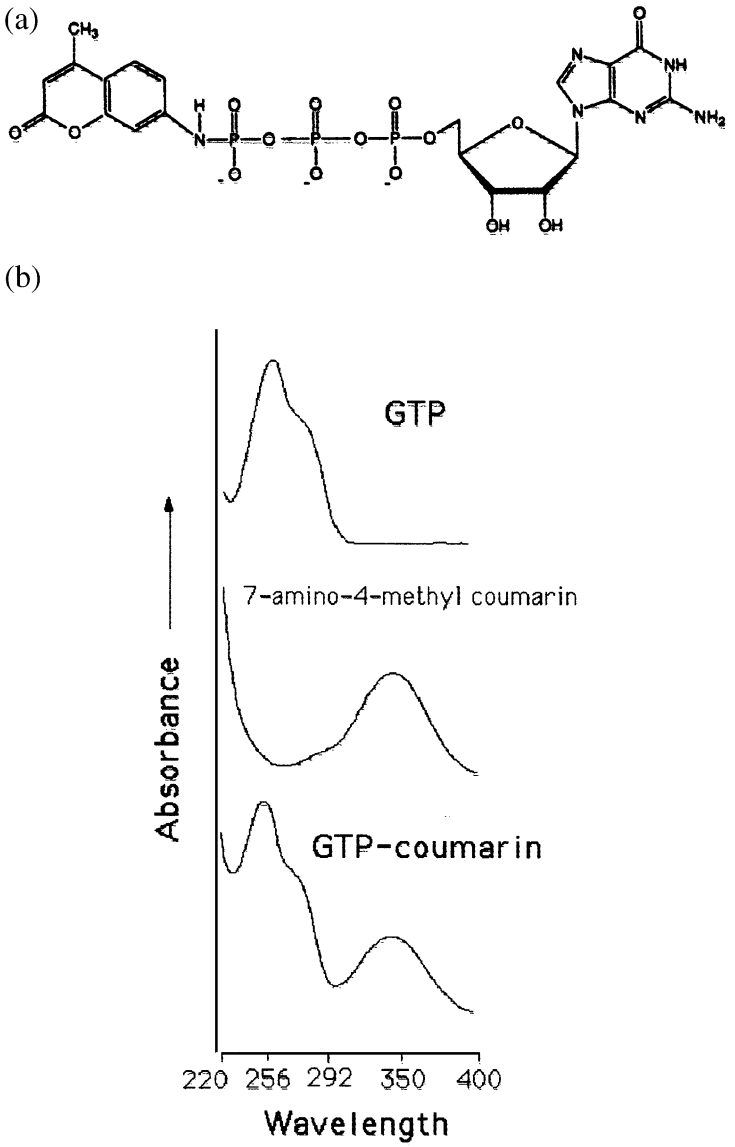

Fig. 1. (a) Structure of Cm-GTP. (b) Comparative UV-VIS absorption spectra of GTP (top), Cm (middle) and Cm-GTP.

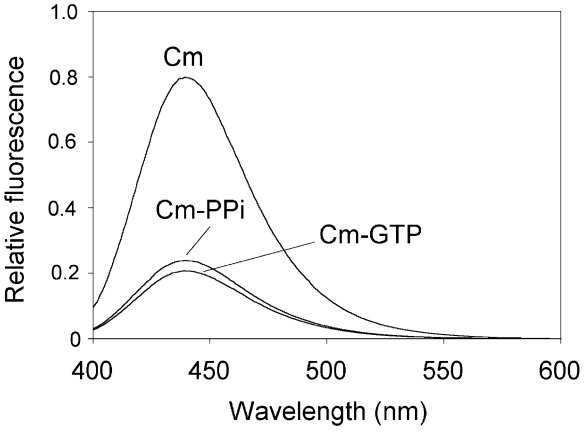

Fig. 2. Emission spectra of Cm, Cm-PP_i and Cm-GTP. Excitation was at 350 nm.

by absorption/fluorescence spectra (Figs. 1 and 2) and by polyethyleneimine-cellulose TLC. The final product was visible as a single spot under UV illumination of TLC plates, which were developed at room temperature with NH_4COO^- (pH 10.5). The product was greater than 98% pure Cm-GTP. Cm-GTP was stored in $MeOH/H_2O$ (50% v/v) at −20°C. The synthetic reaction was a facile one with no stable intermediates as indicated by TLC.

2.2. Digestion with phosphodiesterase

One to two micromoles Cm-GTP was suspended in 700 μl of 110 mM Tris–HCl (pH 8.9) + 20 mM $MgCl_2$ + 100 mM NaCl and the emission spectrum was taken by excitation at 340 nm (see below). Thirty micrograms of *Crotalus adamanteus* crude venom phosphodiesterase I (Sigma) was added and the reaction was incubated at 37°C for 6–8 h. The reaction was clarified by centrifugation in a microfuge and the supernatant was transferred to a cuvette and the emission spectrum was recorded. Under the conditions of digestion > 90% of Cm-GTP was hydrolyzed, as checked by TLC.

2.3. Fluorescence spectroscopy

Steady-state intensity spectra and anisotropy data were acquired by using a JOBIN YVON/SPEX fluorolog (Instruments, S.A. Inc., NJ) equipped with polarizers. Lifetime data and phase angles for anisotropy decay were acquired with the fluorolog 3 τ model (SPEX). Steady-state/anisotropy measurements were made at 37°C whereas, lifetime and anisotropy/anisotropy decay data were acquired at 23°C because lifetimes of reference compounds were reliable only at room temperature. The instruments were calibrated by using Xe lamp intensity spectra and water Raman emission spectra before all experiments commenced. The reference and experimental samples were loaded in temperature-controlled fused quartz square cuvettes (0.7 or 1.0 ml) that were held in a rotary turret with constant stirring. For steady-state data acquisitions, the excitation was usually at 340 nm and the emission was either at 450 nm or in the indicated range with the monochromator bandpass set at 5 nm. Each final scan was an average of two or three individual scans. Spectra were corrected for wavelength-dependent Xe lamp output intensity fluctuation and photomultiplier response by using a reference detector. Measurements were taken in 0.6–1.0 ml (final) of transcription buffer (30 mM Hepes pH 7.8, 100 mM K^+ Glutamate, 15 mM Mg $(OAc)_2$, 1 mM DTT, 0.05% Tween-20, [20]) containing a constant concentration of Cm-GTP (+unmodified NTP) and different concentrations of T7 RNAP. Additions of T7 RNAP storage buffer had no effect on fluorescence intensity. For the extrinsic quenching experiments, the quencher was added to the reactions by using concentrated stock solutions to minimize volume changes (5–10%-change in the total volume). The Stern–Volmer quenching constant was calculated by using the equation in [21]: $F_0/F = 1 + K_{sv}[Q]$, where F_0 and F are the fluorescence intensities with and without the quencher, respectively, K_{sv} is the Stern–Volmer quenching constant and $[Q]$ is the concentration of quencher. The bimolecular quenching constant was calculated from the relation [21]: $k_q = K_{sv}/\langle\tau\rangle$, where k_q is the bimolecular quenching constant and $\langle\tau\rangle$ is the intensity-average fluorescence lifetime of the fluorophore (6.14 ns).

Anisotropy was measured by using the L-format

method [1]. The excitation and emission monochromators were set at 340 and 450 nm, respectively. The alignment of the polarizers was checked by using magic angle (54.7°, anisotropy = 0) and a dilute solution of glycogen in water, as a scattering agent (anisotropy = 0.99863). The G-factor was measured and the data were auto corrected for dark current. Anisotropy was calculated by a computer program (SPEX) by using Eq. (1):

$$r = (I_{VV} - GI_{VH})/(I_{VV} + 2GI_{VH})$$

where, I is the fluorescence intensity with polarizers oriented either vertically (V) or horizontally (H), the first and second letters indicate the excitation and emission polarizer orientations, respectively and $G = I_{HV}/I_{HH}$, which is a correction factor for the different transmission efficiencies of the emission monochromator for vertically and horizontally polarized light. Each anisotropy value was the average of five independent measurements (S.E. = 0.1%).

Average lifetime [$\langle\tau\rangle$] was acquired by using the phase-shift and demodulation method [1]. The standard-lifetime compounds were: *p*-Terphenyl (lifetime 1.0 ns); and 1, 4-bis[5-phenyl-2-oxazolyl]benzene (lifetime 1.3 ns). A scattering agent, glycogen in water (0-ns lifetime) was used to correct for baseline fluctuations during lifetime acquisition. Lifetimes of the experimental samples were measured against 1, 4-bis[5-phenyl-2-oxazolyl]benzene in MeOH. Excitation was at 340 nm and emission was measured by using the T-detector fitted with a neutral density filter (KV 399, Schott) to cut-off stray light below 399 nm. The AC/DC signals were balanced for the reference and for the experimental samples. Fifteen modulated excitation frequencies ranging from 10 to 200 MHz were synthesized. A minimum of five and a maximum of 10 repeat measurements of phase and demodulation were taken. The intensity-average lifetime was calculated from the fractional amplitude (α) and lifetime (τ) using both the phase-shift and demodulation data. Post-experiment lifetime modeling program version 2.1 (SPEX) was used to fit the data to a double-exponential decay model, giving fits with good χ^2 values (1.1–1.9). Fitting the lifetime data to a single-exponential model gave unacceptable χ^2 values.

Time-dependent anisotropy decay was measured by differential polarized phase fluorometry. In practice, this technique is similar to the lifetime acquisition procedure described above, except that the modulated excitation and emission are measured through polarizers. The fluorophore in transcription reactions was excited through vertically positioned polarizers with frequency-modulated 340-nm light. The phase angle of the emission was measured with polarizers oriented either parallel or perpendicular relative to the vertically polarized excitation by using the T-detector fitted with the neutral density filter (see above). The phase difference is given by $\Delta = \phi_{\perp} - \phi_{\parallel}$, where, $\phi_{\perp}$ is the perpendicular component of the phase angle and $\phi_{\parallel}$ is the parallel component of the phase angle of the emission. The phase differential is an indirect measure of the anisotropy decay $r(t)$ because it is sensitive to the rate of fluorophore rotational depolarization. The rotational correlation times were obtained by fitting the phase data to a three-exponential model using anisotropy decay modeling program version 2.2 (SPEX).

3. Results

3.1. Synthesis and characterization of Cm-GTP

A coumarin fluorophore was attached to the γ-phosphate of GTP by using a well-defined coupling method (Fig. 1a). This facile coupling reaction occurred without stable intermediates and yielded coumarin conjugation to the γ-phosphorus position in GTP. The Cm-GTP derivative was characterized by polyethyleneimine-cellulose thin layer chromatography (Cm-GTP $R_f = 0.43$, GTP $R_f = 0.75$, data not shown), UV-absorbance (Fig. 1b) and fluorescence (Fig. 2). Cm-GTP was purified from unmodified compounds by DEAE-sepharose chromatography followed by HPLC. The absorption spectrum of purified Cm-GTP bore the characteristic coumarin peak centered at 343 nm, which was less intense than the corre-

sponding peak from free Cm. And the slightly blue-shifted peak (250 nm) represented the guanine base (Fig. 1b). The fluorescence spectrum of Cm-GTP showed an emission band centered ~ 440 nm, which is characteristic of Cm (Fig. 2). There was a three-fold decrease in emission intensity from Cm-GTP ($\Phi_F = \sim 0.004$) as compared to that from free Cm ($\Phi_F = 0.01$) and very little change (~ 2-nm red shift) in the emission maximum (Fig. 2). A product of transcription with Cm-GTP is Cm-PP_i, which was generated by cleavage of Cm-GTP with venom phosphodiesterase I [3,4]. The fluorescence of Cm-PP_i was only slightly more intense (~ 10–15% higher intensity at λ_{max}) than that of Cm-GTP (Fig. 2). The UV-VIS absorption spectra of the sample of Cm-GTP digested with phosphodiesterase showed a corresponding increase in the absorption peak centered at 343 nm (not shown). However, there was no shift in the absorption maximum for the Cm moiety. These results indicated that the apparent fluorescence quantum yield of the two Cm derivatives (Cm-GTP and Cm-PP_i) were more or less the same.

3.2. Transcription with fluorescent nucleotide

To test if Cm-GTP was a substrate for T7 RNAP, I performed transcription by using a G-ladder RNA slippage synthesis assay, which contained unlabeled Cm-GTP mixed with trace amounts of [α-^{32}P]GTP. The plasmid DNA template *p*Bluescript, which was used in this assay, has a T7 RNAP promoter, which initiates with GGGCGAA etc. With only Cm-GTP (and/or unmodified GTP) a G-ladder was synthesized by T7 RNAP in a slippage reaction (Fig. 3a). This result shows that Cm-GTP is efficiently utilized by T7 RNAP to incorporate GMP into RNA. In this reaction, because the concentration of Cm-GTP (or GTP) is much greater than the concentration of [α-^{32}P]GTP most of the GMP comes from Cm-GTP (or GTP) (Fig. 3). The enzyme active site (3′ RNA terminus) undergoes slippage between position +1C to +3C on the template [12]. The G-ladder with Cm-GTP was similar to that with unmodified GTP, except that the individual RNA rungs appeared to have slightly slower mobilities compared to their normal counterparts because the 5′ end of the RNAs contained a Cm-GTP instead of an unmodified GTP (Fig. 3a). Thus, Cm-GTP was a good substrate for T7 RNAP. To compare the utilization of Cm-GTP with its natural counterpart, GTP, I mixed equimolar concentration of the two nucleotides in the same transcription reaction. Because the modified and unmodified G-ladders have different apparent mobilities, one sees them as distinct doublet bands in the same lanes (Fig. 3b, lanes 3 and 4). The upper band in each doublet corresponds to the RNA with 5′ Cm-GTP whereas, the lower band is the unmodified RNA. In this competition assay, it appears that both Cm-GTP and GTP were incorporated by T7 RNAP in a quantitatively similar manner. Quantitation of the intensities of the doublet bands in Fig. 3b (lanes 3 and 4) suggested that the amount of incorporation of Cm-GTP was only slightly lower (by $2-3x$) relative to GTP. This difference, when translated into kinetic constants (~ few-fold change in K_m and V_{max}) between Cm-GTP and GTP is not significant, especially under the steady-state transcription conditions used in this work where the nucleotide concentrations were not limiting.

Because a modified form of GTP was incorporated into RNA, it was important to test if RNAP-RNA interactions could contribute to changes in fluorescence (see below). In other words, the stability of RNA in ternary complexes could affect changes in fluorescence. To test the stability of RNA + RNAP complexes, a membrane filter-binding assay was used [22]. The results indicated that complexes with longer RNA (14 mer) were the most stable (Fig. 3b, lane 1). (Note, free RNA was not retained in the filter-binding assay). Addition of SDS disrupted the stable complexes indicating that the transcript was bound to protein (T7 RNAP) (Fig. 3, lane 2). A longer exposure of the X-ray film revealed that complexes containing 10–14 mer RNAs were more stable than the shorter ones. These results are in qualitative agreement with a previous report [23]. Approximately 10% of the incorporated ^{32}P in RNA were retained as 14 mers and above,

and 80% of these T7 RNAP-RNA complexes were retained on the filters. These molecules are a minor fraction (< 1–2%) of the total number of RNA molecules in the reaction. Thus, in the total mixture of RNAs being synthesized under steady-state conditions, only a very small fraction of RNAs in the range of 10–14 mers are stably bound to the enzyme. Most of the RNA produced during poly-G ladder synthesis must be free.

I also examined the rate of abortive initiation and the stability of abortive initiation complexes. With *p*Bluescript template and Cm-GTP (plus a trace amount of [α-^{32}P]GTP) + CTP + ATP, T7 RNAP synthesizes up to 7-mer RNAs (5′GG-GCGAA) because UTP, which is required at the eighth position, is missing. Under these conditions, abortive initiation occurred with high frequency, and transcripts up to 7-mers and, to a much lesser extent longer ones, were observed (Fig. 4a). The longer transcripts may have arisen owing to traces of UTP generated via spontaneous cytosine deamination or from a minor transcription pathway in which, slippage was followed by extension (3 + 7). (Note: the length assignment for abortive transcripts was based on comparisons with a more extensive previous study [23].) Fig. 4b (lane 3) shows that abortive RNAs were retained in the filter binding assay with only very low efficiency and with no specific length preference. Thus, in the abortive initiation reaction as well, most of the RNA containing the fluorophore must be free.

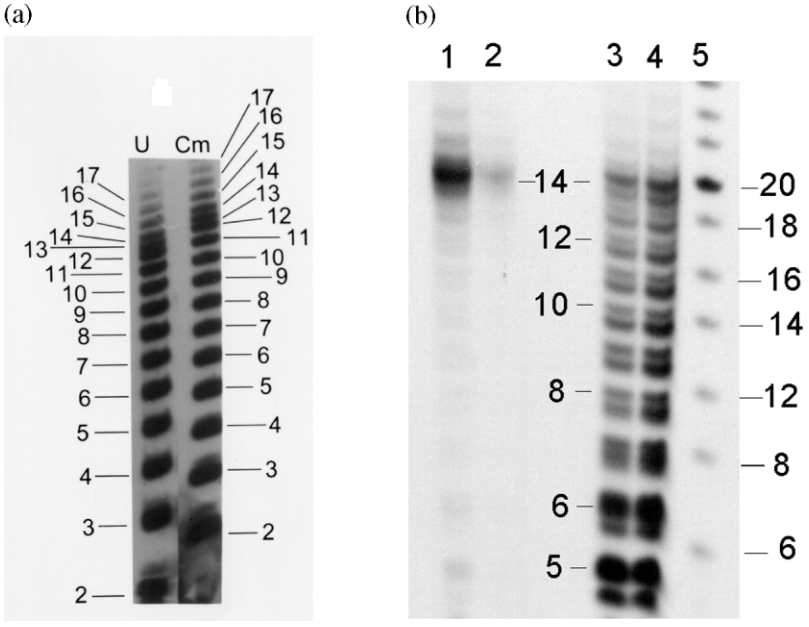

Fig. 3. (a) Denaturing urea-acrylamide gel showing G-ladder synthesis using either unmodified GTP (U) or Cm-GTP (Cm). The numbers indicate the length of RNAs in the ladders. GTP and Cm-GTP were unlabeled (~ 1 mM) and [α-^{32}P]GTP was used as a tracer (0.7 μM). (b) Stability of G-ladder complexes was tested by using a PE81 (Whatman) filter-retention assay. The filters were mounted on a filtration device, washed with water and then wetted with 2 ml of transcription buffer. Thirty minute transcription reactions (50 μl) were then applied to the filter without suction and the filter was washed with 5 ml of transcription buffer under gentle suction. To elute the bound RNA, the filters were then transferred into a 200-μl solution of 1% SDS + 50 mM EDTA at 37°C for 1 h. The eluted RNA was precipitated with EtOH and sodium acetate. The RNA samples were run on a denaturing urea-acrylamide gel. Lane 1 shows filter-bound RNAs and lane 2 shows filter-retained RNAs following the addition of SDS to the complexes. Lane 3 and 4 are transcription reactions with equimolar concentrations (~ 50 μM) of Cm-GTP and GTP in the same reaction. Lane 3 contained lesser amounts of radioactivity than in lane 4. Lane 5, DNA markers, numbers between lanes 2 and 3 indicate the length of G-ladder. Numbers on the right indicate the sizes of the DNA markers.

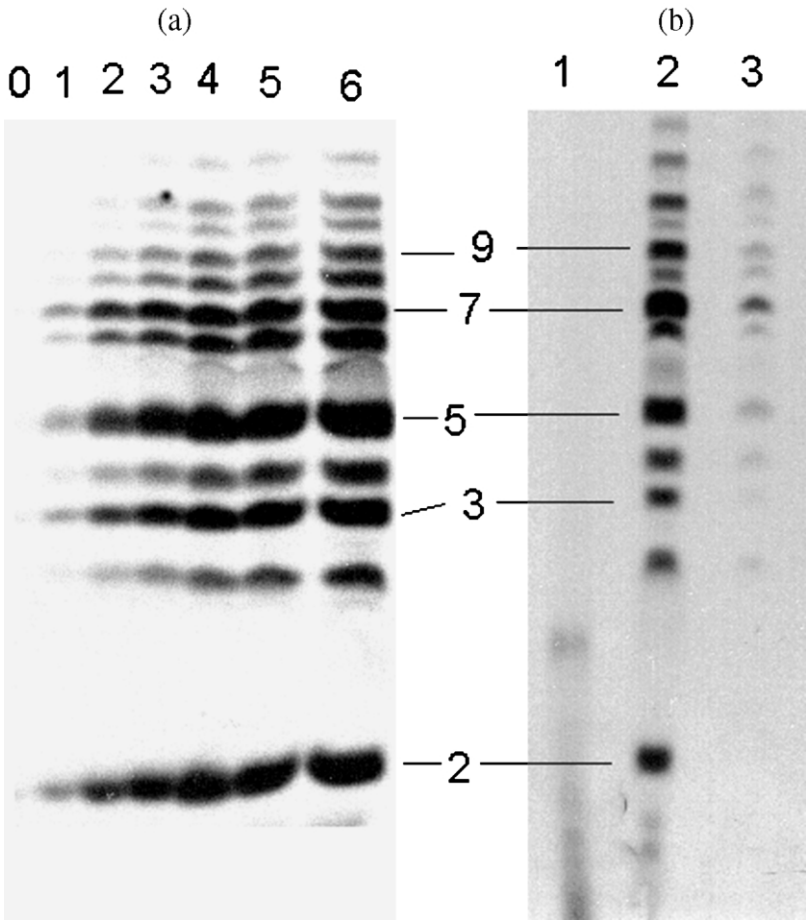

Fig. 4. Time course of abortive transcription (a) and stability of abortive transcripts (b). Panel A: time course; lanes 0 through 6, are 0, 0.5, 1, 5, 15, 25 and 40 min, respectively. Panel B, PE81 filter-retention assay for ternary complex stability. Lane 1: control, no transcription; lane 2: abortive transcripts before filtration; and lane 3: shows filter-retained abortive transcripts. The numbers between the panels indicate the length of abortive transcripts.

3.3. Fluorescence assay for transcription

Addition of increasing amounts of T7 RNAP to Cm-GTP under conditions of transcription resulted in decrease in the fluorescence intensity (Fig. 5a). Here, Cm-PP_i was being generated as Cm-GTP was consumed. There are three species of fluorophores viz., Cm-GTP, Cm-PP_i and RNA-incorporated 5′ Cm-GTP. Because the relative fluorescence intensity (and hence quantum yield) of Cm-GTP and that of Cm-PP_i were nearly the same (Fig. 2), hydrolysis of nucleotide was ruled out as the cause of quenching. (There was no apparent difference in fluorescence intensity between transcription buffer and phosphodiesterase buffer and a change in intensity-averaged lifetime was also ruled out, see below.) A time scan of fluorescence signal after the addition of T7 RNAP (t_0) showed that there was a gradual decrease in fluorescence intensity as transcription occurred (Fig. 5b), but essentially no change when T7 RNAP was omitted (not shown). Fig. 5c shows that under conditions similar to those employed in the fluorescence assay, G-ladder synthesis occurred in a stoichiometric manner with each addition of T7 RNAP and that transcript synthesis

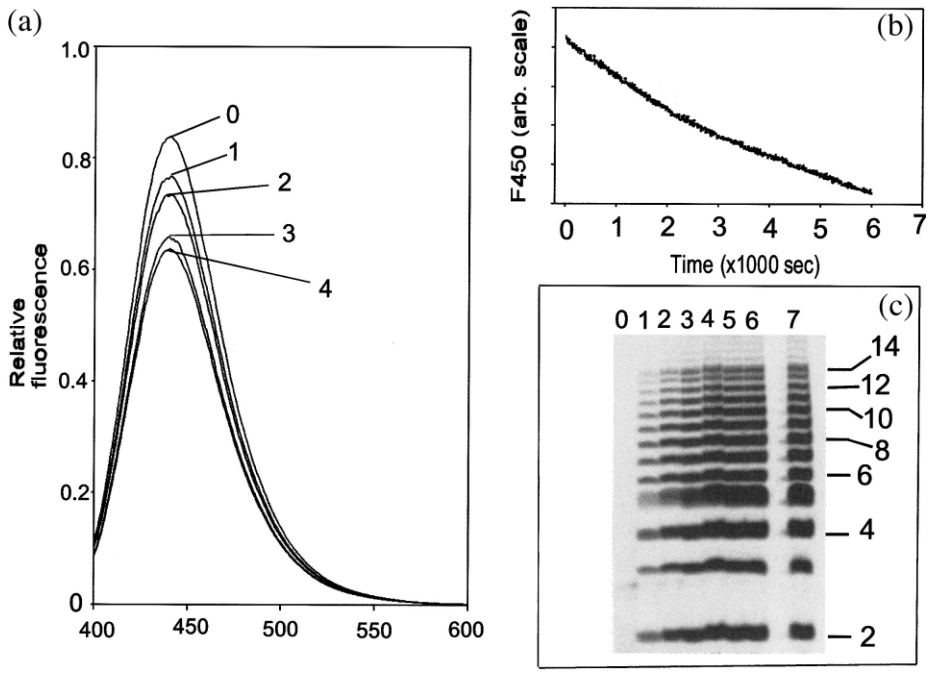

Fig. 5. Panel A: fluorescence assay for Cm-GTP incorporation by T7 RNAP during G-ladder transcription. Curves 0–4 are with 0, 0.5, 0.75, 2 and 2.5 μM T7 RNAP, respectively. Higher enzyme concentrations were not tested because of the rise in interference from light scattering. Standard transcription reactions (15 min) contained either Cm-GTP (~30 μM) + unlabeled GTP (500 μM) or Cm (~20 μM) + *p*Bluescript DNA template (3 μg) in transcription buffer (see Section 2). Panel B: change in fluorescence intensity following the initiation of transcription (t_0). Transcription reaction contained T7 RNAP (3 μM) and 1 mM GTP + 30 μM Cm-GTP. The fluorescence of the reaction was continuously monitored at 450 nm ($E_x = 340$ nm). Panel C: G-ladder synthesis assay. Assay conditions were similar to those used in the fluorescence assay of panel A except that the reactions contained a trace amount of [α-^{32}P]GTP. Lanes 0 through 7 indicate concentrations of T7 RNAP used, 0, 0.5, 1, 1.5, 2.5, 4, 6 and 7 μM, respectively. The numbers on the right side indicate the length of the G-ladder.

was complete within the time scale of the fluorescence assay. In control experiments using Cm alone with T7 RNAP, the fluorescence intensity did not change (not shown). Thus, T7 RNAP and nucleotide-incorporation into RNA were necessary for the observed intensity changes. Omission of DNA template from the transcription reaction resulted in a very insignificant decrease (4–5%) in fluorescence. This was presumably due to non-specific binding or binding at the initiation site. However, no time-dependent decrease was observed, in contrast to the experiment shown in Fig. 5b. Together, these results substantiate the finding that fluorescence was quenched because Cm-GTP was incorporated in to poly-G RNA ladders.

Because the rate of Cm-GTP utilization was similar to that of GTP (Fig. 3), it was estimated that approximately 30% of Cm-GTP was consumed. This was determined by spiking the reaction with [α-^{32}P]Cm-GTP. Approximately 8–10% of the input Cm-GTP was incorporated at the 5′ end of RNA. This estimate was done using [γ-^{32}P]GTP, which, like Cm-GTP, is only incorporated at the 5′ end of RNA. These are upper limit estimates because GTP is slightly better than Cm-GTP as a substrate. In the transcription reaction with Cm-GTP, there was Cm-PP_i (both enzyme-bound and free) and 5′ RNA-incorporated Cm-GTP. The fluorescence intensity (and hence the apparent quantum yield) of free Cm-PP_i was not significantly different from that of free

Cm-GTP (Fig. 2). The binding of PP_i in the active site of the polymerase is quite weak and transient [24]. Therefore, it is unlikely that enzyme-bound Cm-PP_i could have contributed significantly to fluorescence quenching. The filter-retention assay showed that RNA molecules only in the size range of 10–14 mer were stably bound to T7 RNA polymerase (Fig. 3). The fraction of Cm-GTP at the 5′ end decreases with increasing length of the poly-G ladder. The fraction of Cm-GTP at the 5′ end of these molecules is very small ($< 1\%$) compared to the majority Cm-GTP at the 5′ end of poly-G RNAs in the 2–9 mer size. Thus, the quenching of fluorescence cannot be attributed to the polymerase-bound poly-G ladder either because under steady-state transcription, this fraction is very small and constant (Fig. 3b). Thus, some fluorescence quenching (Fig. 5a) is due to incorporation of Cm-GTP in RNA.

I repeated the fluorescence assay under conditions of abortive cycling. Under these conditions abortive transcripts up to 7 or 8 nts were synthesized in a stoichiometric manner (Fig. 6b). However, in the fluorescence assay there was much less decrease (only up to $\sim 6\%$, Fig. 6a) in fluorescence intensity than had been seen with the G-ladder synthesis ($\sim 25\%$, Fig. 5a). In both G-ladder synthesis and abortive modes, regardless of RNA length, each RNA molecule carries only one fluorophore, Cm-GTP at its 5′ end. However, the RNAs made in abortive cycling reactions did not contain as many rGs (only 3 rG in a row per molecule). The difference in the degree of fluorescence quenching in G-ladder synthesis vs. abortive initiation assay must be due to differences in microenvironment of the fluorophore. I suggest that this is because the poly-G RNA ladders may adapt unusual conformation such as

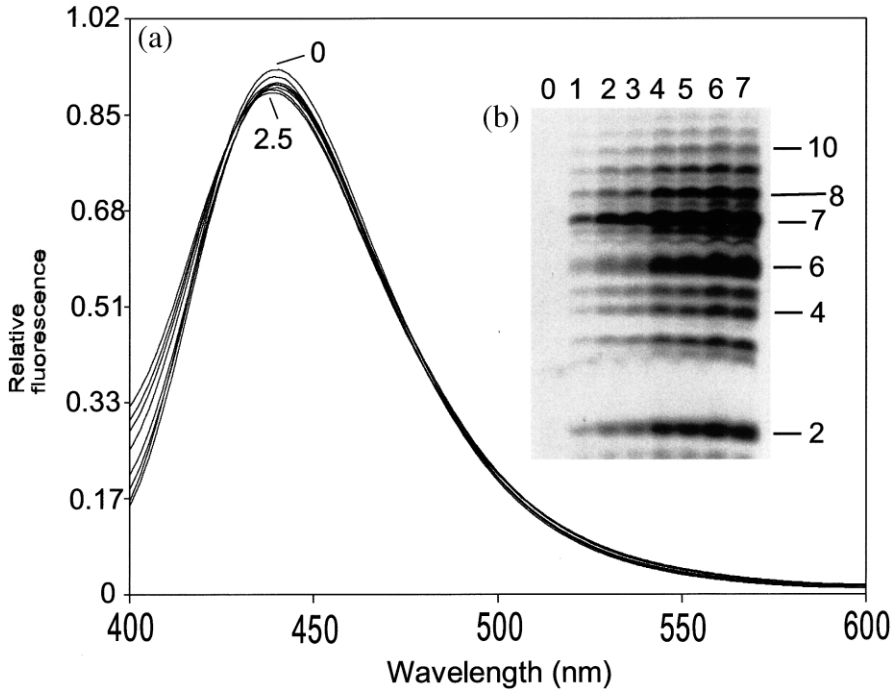

Fig. 6. Panel A: fluorescence assay for abortive transcription with Cm-GTP + GTP + CTP + ATP. Conditions for transcription and spectra acquisition were similar to those in Fig. 5. The concentrations of CTP and ATP were 1 mM. The curve numbers (0, 2.5) indicate the concentrations (μM) of T7 RNAP used. The intermediate curves were generated using 0.2, 0.4, 0.8, 1.0, 1.2, 1.4 and 2.0 μM T7 RNAP. Panel B: abortive transcription assay. Assay conditions were similar to the fluorescence assay in panel A except that the reactions contained a trace amount of [α-^{32}P]GTP. Lanes 0 through 7 indicate concentrations of T7 RNAP used, 0, 0.5, 1, 1.5, 2.5, 4, 6 and 7 μM, respectively. The numbers on the right side indicate the length of the abortive transcripts.

G-quartets [13,14] and the abortive RNAs do not (see Section 4).

To better understand the photophysical basis for the decrease in fluorescence intensity in G-ladder reactions, I measured the average lifetime (Fig. 7). The intensity-average lifetime of free Cm-GTP [$\langle\tau\rangle = \sim 5$ ns] was slightly longer than the reported lifetime values for Cm (note, τ for Cm is < 2 ns in organic solvent [25,26]. Due to low solubility, τ in aqueous buffer has not been measured). However, more importantly, the intensity-weighted average lifetime [$\langle\tau\rangle = 6.14$ ns] of the fluorophore was the same under various transcription conditions (hence all the data sets are not shown here, see Fig. 7 for a sample data set). Here, the fluorescence is dominated by a single component ($\alpha_2 = 0.87$) with a longer lifetime (4.72 ns). This is probably because the lifetime differences, if any, of the components in the transcription reactions, Cm-PPi and Cm-GTP in RNAs, were too small to be resolved and only an average value was obtainable. Hence, it is likely that the average lifetime is a composite value from all the species in the transcription reaction. The concentration of coumarin molecules in transcription reaction does not change. However, the fluorescence (intensity) quantum yield is not an energy ratio but it is related to non-radiative processes [$(\Phi_F = \Gamma/\Gamma + \Sigma k_i)$ where, Γ is the rate of radiative decay and Σk_i is the sum of all rates of non-radiative decay processes]. Because there was no change in the average lifetime (~ 6 ns) during transcription, the fluorescence quenching during G-ladder synthesis (Fig. 5) must be due to static or quasi-static quenching (ground-state heterogeneity), thereby accounting for the lower apparent quantum yield due to non-radiative decay processes. But how can an 8–10% incorporation of Cm-GTP in 5′ RNA produce $\sim 25\%$ quenching effect even if we assume that all the incorporated Cm is in ground-state non-fluorescent complex? It is possible that additional dynamic (collisional) quenching processes that depopulated the excited state may have occurred. These may involve small decreases in lifetime (that I could not detect). Clearly, more photophysical experimentation is needed to clarify the mechanism of quenching.

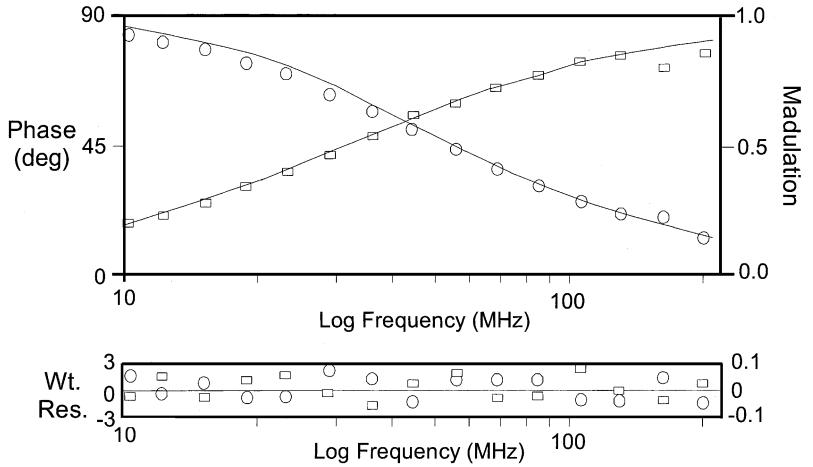

Fig. 7. Frequency-domain fluorescence lifetime modeling. Top panel: phase (boxes) and modulation (circles) data were fitted to a two-exponential lifetime model. The lines indicate the fit of the data. Lower Panel: the goodness of fit was assessed using the random distribution of weighted residuals, which corresponds to the difference between the experimental and calculated values normalized by the experimental errors for the phase and demodulation. The typical lifetime decay parameters for G-ladder synthesis: $\alpha_1 = 0.12$; $\tau_1 = 0.76$; $\alpha_2 = 0.87$; $\tau_2 = 4.72$; $\langle\tau\rangle = 6.14$; $\chi^2 = 1.79$, where α is the fractional amplitude associated with each lifetime (concentration of the component, pre-exponential factor), τ is the lifetime in ns. The χ^2 value indicates the goodness of fit, $\langle\tau\rangle$ is the intensity-average lifetime in ns, which was calculated using the expression $\Sigma\alpha_i\tau_i^2/\Sigma\alpha_i\tau_i$.

However, because my focus is to demonstrate the usefulness of the new fluorescent probe, I did not further pursue this line of work.

Alternatively, it is possible that fluorescence intensity decreased because of the high purine content of G-ladder RNA. Fluorescence quenching in purine rich oligonucleotides due to nearest neighbor effects is well known (e.g. [9,27]). However, in our case, this explanation is unlikely because: (1) the fluorophore is in a terminal position; and (2) the nearest neighbors in the G-ladders as well as in the abortive transcripts are the same purines (GGG). Thus, differences between G-ladders and abortive transcriptions in terms of the magnitude of fluorescence quenching are not due to RNA sequence differences per se but due to differences in RNA conformation.

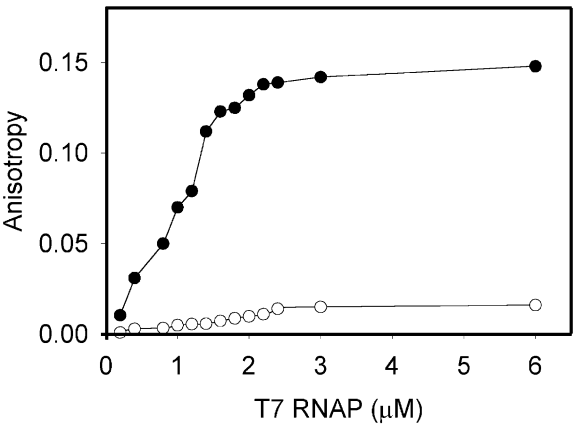

Fig. 8. The change in steady-state anisotropy during G-ladder synthesis (filled black circles) or during abortive RNA synthesis (empty circles) as a function of T7 RNAP concentration.

3.4. Rotational dynamics of fluorophore in poly-G ladders

To gain further insights into the microenvironment of the fluorophore in transcription reactions, I measured steady-state anisotropy and anisotropy decay. Anisotropy is related to the rotational diffusive motions of the fluorophore during the lifetime of the excited state, which indicates the viscous drag imposed on the fluorophore [1]. Anisotropy measurements do not require the separation of bound fluorophore from the free fluorophore. Anisotropy is sensitive to increasing molecular mass and changes in macromolecular conformation.

During G-ladder transcription, steady-state anisotropy increased with T7 RNAP concentration (Fig. 8). As shown previously, with higher concentration of polymerase there was greater accumulation of poly-G molecules (Fig. 5). Anisotropy data suggested that with increasing concentration of poly-G more complex conformers could have formed. The 5′ fluorophores in RNA G-ladders were held in a more rotationally constrained environment, perhaps due to special conformational features of poly-G ladders (G-quadruplexes). To rule out the possibility that a very small fraction of enzyme-RNA interactions contributed to anisotropy, a control experiment was done. The G-ladder transcription reactions were deproteinized by SDS-phenol extraction and EtOH precipitation and the anisotropy of the sample was measured. The anisotropy (0.12) was equivalent to that during G-ladder synthesis reactions. This indicated that the rotation of fluorophore was indeed constrained in poly-G ladder RNAs.

In contrast to poly-G ladders, under conditions of abortive transcription there was very little change in anisotropy with increasing concentration of abortive transcripts (Fig. 8). [Note, under both conditions there was robust RNA synthesis (Figs. 5 and 6).] This indicated that abortive transcripts did not form complex structures.

To further assess the rotational dynamics of the fluorophore during transcription, I measured frequency-domain fluorescence anisotropy. The rate of fluorophore rotation is related to the steric hindrance. To determine the rate of rotational motion of fluorophore, I measured differential phase angles between 10 and 200 MHz (the data acquisition format is similar to that in Fig. 7). There was a continuous rise in the differential phase angle with an increase in modulation frequency (Fig. 9). The phase data were fit to a three-component model (Fig. 9). In the absence of data from model or purified components, it is difficult to assign the correlation times to rotational depolarizing motions of any specific molecular

species in the transcription reaction. However, the longer rotational correlation time $\phi_2 = 4.9$ ns may be associated with poly-G of median size of 7 or 8 mer (mol. wt. = ~ 3 K). The predicted correlation time ($\phi = \eta V/RT$, where η is viscosity, V is volume of rotating unit) for a rigid anhydrous sphere of a similar molecular weight is ~ 2–3 ns. Generally, the observed ϕ is twice that expected for an anhydrous sphere. The larger observed ϕ value is probably due to the non-spherical nature of RNA and greater hydration. G-Quartets are not spherical but they are symmetric (see Fig. 11b), which may explain to some extent the closeness of the observed and calculated ϕ values.

The anisotropy data do confirm the presence of large molecular structures. To cross-check the anisotropy decay, I used the Perrin equation [1], $r = r_0/1 + (\tau/\phi)$ (where, r is the anisotropy, r_0 is the anisotropy at time zero (limiting anisotropy, i.e. no rotation), τ is the average lifetime and ϕ is the rotational correlation time). I estimated $r =$ 0.145, a value close to the observed steady-state anisotropy value (Fig. 8).

The large χ^2 value (Fig. 9) indicated that the three-exponential anisotropy decay model does not fit the data satisfactorily, probably because there were additional rotational motions associated with the depolarization process, which were not resolved. Adding a fourth exponential did not significantly improve the goodness-of-fit parameter. However, greater than two-fold decrease in χ^2 value in going from a two-component to a three-component model suggested that the later is an improved fit for the decay model.

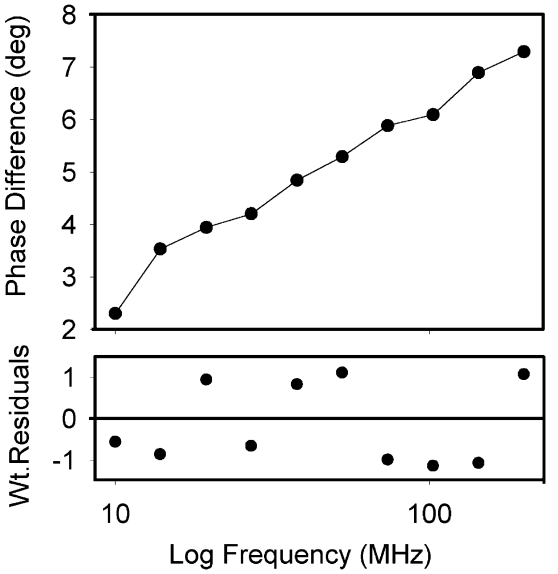

Anisotropy Decay parameters

β_1	ϕ_1	β_2	ϕ_2	β_3	ϕ_3	χ^2
0.13	1.1	0.17	4.97	0.02	0.12	2.2

Fig. 9. Anisotropy decay model for G-ladder reactions. Top panel: differential phase angle as a response to frequency. The lower panel shows the random distribution of weighted residuals, which represents the difference between the experimental and calculated values normalized by the standard error. The anisotropy decay parameters are shown in the bottom panel. β_i is a pre-exponential term that represents the extent to which the emission is depolarized by each rotational component $\Sigma\beta_i = r_0$ (0.32) and ϕ_i is the rotational correlation time. The χ^2 value indicates the goodness of fit.

3.5. Fluorescence quenching by using extraneous reagents

Fluorescence quenching by using an extraneous quencher provides an effective means of gaining information regarding solvent accessibility of the fluorophore [1,21]. Iodide was used as the negative ion quencher, thallium as the positive ion quencher and acrylamide as the neutral/polar quencher (Fig. 10). The Stern–Volmer quenching constant (K_{sv}) and the bimolecular rate constant (k_q) were calculated (see Section 2 Table 1). Stern–Volmer plots were linear and were significantly different for G-ladder synthesis conditions as compared to the free Cm-GTP (Fig. 10). The relative efficiency (K_{rel}) of quenching by extraneous quenchers suggested that collisional quenching was drastically reduced in G-ladder transcription reactions (Table 1). The shielding of fluorophore in poly-G ladders may have contributed to this effect (see Section 4). The bimolecular rate constants (k_q) for iodide, acrylamide and thallium were at the diffusion limit (Table 1). This makes sense because the major species in the transcription reaction are the free Cm-GTP

and free Cm-PP_i and RNA containing 5′ Cm group. Our data are consistent with a model of a small organic molecule (5–8 Å radii) being efficiently quenched (theoretical rates, $5 \times 10^9 - 1 \times 10^{10}$ M^{-1} s^{-1} [21]). With thallium, there is a greater decrease ($\sim 10\times$) in the rate of quenching in the G-ladder transcription reactions compared to the other quenchers. This is consistent with the fact that monovalent cations bind to and stabilize G-quartets [14]. The specific effect of Tl^+ as compared to I^- on the k_q in the G-ladder transcription reaction suggests a role for G-quartets (Table 1).

Upward curvature of Stern–Volmer plot (Fig. 10c) at high [acrylamide] suggests ground state heterogeneity (more than one fluorescent species), perhaps more than one fluorophore microenvironment where quenching occurs by static as well as dynamic mechanisms. There could be transient state/chemically distinct ground state or the probability that the quencher and chromophore are close to each other but are not interacting. Upward trend for Stern–Volmer plot was seen in other systems as well, the quenching of indole by acrylamide [21].

It must be borne in mind that there are several species, RNA incorporated Cm-GTP, free Cm-GTP and Cm-PP_i in the transcription reaction. In addition, there may be multiple conformations in the poly-G ladders. This makes the interpretation less straightforward. Thus, the quenching data may reflect composite values for an entire ensemble of molecules. I cannot apportion the contribution of the individual fluorescent species to the quenching effect. Because in transcription reactions the K_{sv} decreased quite significantly compared to the value for free Cm-GTP (and possibly for Cm-PP_i), the effects in Table 1 are predominantly due to the synthesis of poly-G RNA. Some fluorophores may be in a less solvent accessible microenvironment such as within or close to G-quartets.

4. Discussion

Here I report the synthesis of a new fluorescent analogue of GTP, which can be used in transcription reactions. This analogue can be specifically incorporated at the 5′ end of nascent RNA synthesized by T7 RNAP (and by other RNA polymerases using appropriate templates). The Cm-GTP analogue was used in a different way compared to some previously reported fluorescent analogues [5,6], in which a pyrimidine (UTP) was modified. The analogue I synthesized can be used specifically with T7 RNAP whereas, the others cannot be used with this enzyme to label the RNA 5′ end because T7 RNAP always initiates with an rG residue. T7 RNAP is the preferred enzyme for in vitro synthesis of RNA for structural studies because of its ease of availability and for its rapid rates of RNA synthesis [28]. Cm-GTP

Table 1
Quenching parameters for free Cm-GTP and for G-ladder synthesis

Quencher	Item	K_{SV} (M^{-1})[a]	k_q (M^{-1} S^{-1})[b]	K_{rel}[c]
Iodide				
	Cm-GTP	485.1	7.9×10^{10}	
	+T7 RNAP	79.8	1.3×10^{10}	0.16
Thallium				
	Cm-GTP	178.1	2.9×10^{10}	
	+T7 RNAP	22.1	3.6×10^{9}	0.12
Acrylamide				
	Cm-GTP	448.2	7.3×10^{10}	
	+T7 RNAP	85.9	1.4×10^{10}	0.19

[a] The Stern–Volmer quenching constant.
[b] The bimolecular quenching constant, which were calculated as indicated in experimental procedures.
[c] The relative quenching efficiency, which is defined as K_{sv} Cm-GTP + T7 RNAP/K_{sv} Cm-GTP.

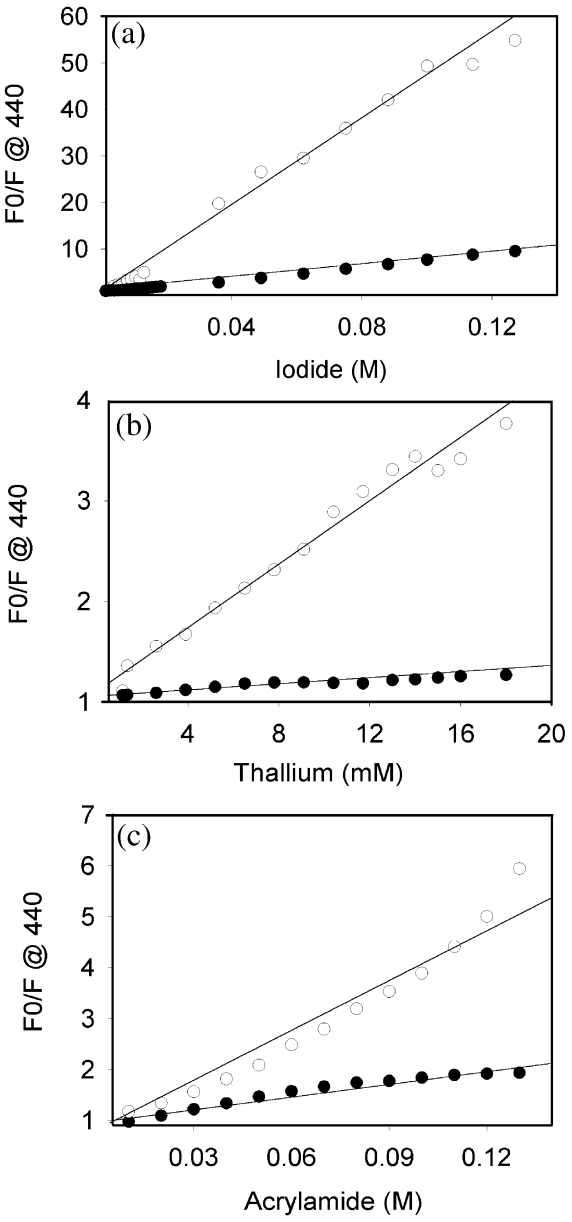

Fig. 10. Stern–Volmer plots for extrinsic quenching (E_x = 340 nm) during G-ladder transcription. Reaction conditions were similar to the fluorescence assay in Fig. 5, except that a single concentration of T7 RNAP (3 μM) was used. F_0 = fluorescence intensity without quencher. F = fluorescence intensity with quencher. No transcription control (empty circles) and G-ladder transcription (filled circles). The lines indicate the fit of the data to the Stern–Volmer equation (see Section 2).

can also be potentially used with *E. coli* RNAP because this enzyme can initiate with GTP on some promoters and under some conditions with low efficiency. The synthetic route can be used to introduce fluorescent label in ATP as well (similar to [17]) which can then be efficiently utilized by *E. coli* RNAP. Thus, the fluorescent probe reported here has potentially wide-ranging utility in RNA structural studies.

I chose the T7 RNAP system to illustrate the usefulness of Cm-GTP as a probe for two reasons. (1) As opposed to some other RNAPs, T7RNAP can initiate transcription in two different ways on its native promoter template. The transcriptions result in RNA products, which have starkly different sequences but with almost similar length distributions viz., poly-G ladders and mixed sequences of abortive RNAs. (2) The sequence of the G-ladders can be readily related to a well known structure i.e. the family of G-quartet conformers. The mixed abortive RNA sequences cannot adopt any known secondary structure and may be assumed to be linear. Therefore, the T7 RNAP system serves as a facile natural example for the study of RNA conformation using fluorescence. The placement of the reporter fluorophore on the γ-phosphorus has allowed the selective labeling of the 5′ end of the nascent RNA and the preclusion of multiple labels in the body of each RNA molecule and non-interference with potential secondary structure formation. Placing the label internally in the body of the transcript or attaching the fluorescent group to the nucleobase would introduce other constraints that might interfere with the natural folding and/or flexibility of RNA. The fluorophore on the 5′ phosphate end of the RNA has a greater degree of rotational freedom (in the absence of secondary structure) than a fluorophore placed internally. The various fluorescence techniques used here demonstrate the feasibility of using the Cm-GTP analogue as a probe for more detailed structural studies of specific RNA sequences.

The observations presented here can be ex-

plained on the basis of the suggestion that poly-G ladders may form G-quadruplex family of configurations (Fig. 11 and reviewed in [14]). G-Quartets arise from single strands of RNA [29] or DNA [30] molecules that associate to form four-stranded structures by a cyclic array of planar guanines involved in hydrogen bonding (Fig. 11a and ref. [14]). There are only two requirements for G-quartet formation (reviewed in [13]). Firstly, a string of at least four consecutive guanine residues in nucleic acid and secondly, a monovalent cation, which serves as a metal ligand for the quadruplex (Fig. 11a). Both requirements are fulfilled in the slippage transcription reactions. It is unlikely that the abortive transcripts, with only three Gs in a row could form G-quartets. This could explain the differences in steady-state fluorescence quenching between G-ladders and abortive transcripts (Figs. 5 and 6). Fluorescence quenching occurred because the 5′ terminal guanine base in Cm-GTP-containing poly-G strands may have been involved in G-quartet formation with other poly-G RNA strands.

Drastically reduced ($\sim 10\times$) collisional quenching during G-ladder synthesis as compared with the free fluorophore-nucleotide (Table 1, K_{rel}) supports the idea that the fluorophore was sequestered. Interestingly, the bimolecular rate constant (k_q) for monovalent cation thallium was much less than with iodide anion (Table 1). Monovalent cations are known to stabilize G-quartets (Fig. 11a). Because K^+ at 100 mM is the predominant monovalent cation in transcription reactions it may uniformly promote G-quadruplex formation. However, this may not exclude a role for Tl^+ ion in mM concentrations in stabilizing the G-quartets in the quenching experiment. The preference between the two ions may depend on the relative ligand binding affinities (which are unknown) of the two ions for G-quadruplexes. In this context, it is interesting to note that *Tl* has a van der Waals atomic radius (~ 200 pm) in the

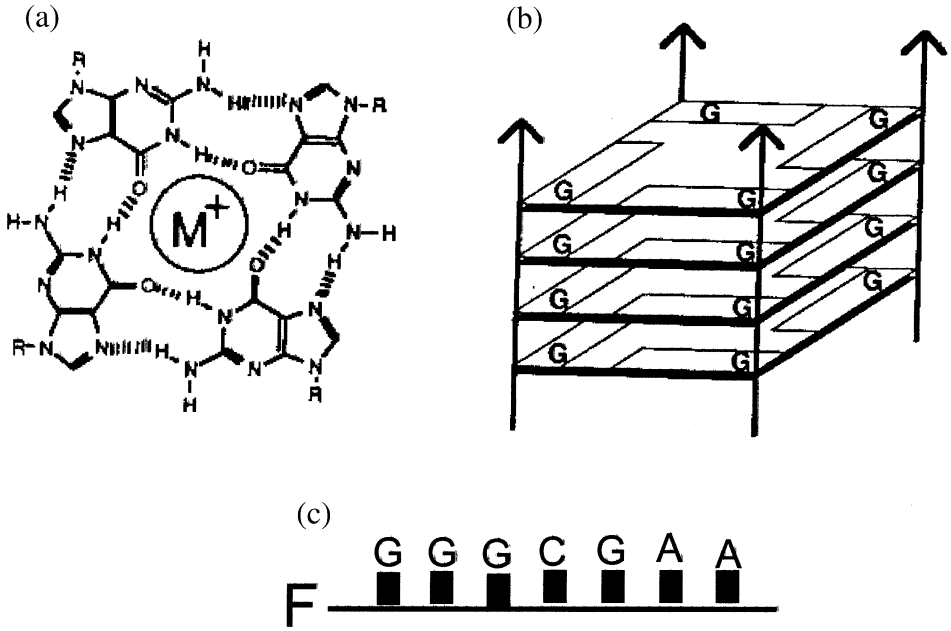

Fig. 11. Proposed configurations for poly-G ladders. (a) System of cyclic H-bonding in a G-quartet structure. *M* is a monovalent metal ligand that stabilizes the G-quartet. (b) Four stranded structure that may be formed in poly-G RNAs in transcription reactions. The arrow suggests the 5′ to 3′ orientation of the G-strands. F is the fluorophore (c) The sequence of the abortive RNA transcripts. Fig. 11a,b were adopted from ref. [14].

vicinity of potassium (atomic radius ~225 pm) and cesium (atomic radius ~250 pm), which are known to bind G-quartets [14].

In conclusion, a new fluorescent GTP analogue has been synthesized and its application in structural studies of RNA synthesized in a natural system using fluorescence spectroscopy has been demonstrated. These studies may pave the way for further insights into RNA structure and conformation using specific RNA sequences synthesized using T7 RNAP.

Acknowledgements

I would like to thank Dr William R. Laws (Mount Sinai Medical Center, New York) for critical comments and suggestions for improvements. This work was supported by research grants from the Cancer Research Institute, New York and from Hewlett Packard Foundation (to S.S.).

References

[1] J.R. Lakowicz, Principles of fluorescence spectroscopy, Plenum Press, New York, 1983, pp. 10, 171–178, 347–357.

[2] J.R. Lakowicz, in: J.R. Lakowicz (Ed.), Topics in Fluorescence Spectroscopy, 3, Plenum Press Publ, NY, 1992, p. 408.

[3] L.R. Yarbrough, Synthesis and properties of a new fluorescent analog of ATP: adenosine-5′-triphosphoro-γ-1-(5-sulfonic acid) naphthylamidate Biochem. Biophys. Res. Comm. 81 (1978) 35–41.

[4] L.R. Yarbrough, J.G. Schlageck, M. Baughman, Synthsis and properties of fluorescent nucleotide substrates for DNA-dependent RNA polymerases J. Biol. Chem. 254 (1979) 12069–12073.

[5] K.S. Dunkak, M.R. Otto, J.M. Beechem, Real-time fluorescence assay for gene transcription: simultaneous observation of protein/DNA binding, localized DNA melting, and mRNA production Anal. Biochem. 243 (1996) 234–244.

[6] M. Hanna, E. Yuriev, J. Zhang, D. Riggs, Probing the environment of nascent RNA in *Escherichia coli* transcription elongation complexes utilizing a new fluorescent ribonucleotide analog Nucl. Acids Res. 27 (1999) 1369–1376.

[7] R.S. Goody, F. Eckstein, Thiophosphate analogs of nucleoside di- and tri-phosphates J. Am. Chem. Soc. 93 (1971) 6252–6257.

[8] R.G. Yount, ATP analogs Adv. Enzymol. 43 (1975) 1–56.

[9] M.E. Hawkins, W. Pfleiderer, P.Y.G. Mazumder, F.M. Balis, Incorporation of a fluorescent guanosine analog into oligonucleotides and its application to a real-time assay for HIV-1 integrase 3′-processing reaction Nucl. Acids Res. 23 (1995) 2872–2880.

[10] T.M. Nordlund, D. Xu, K.O. Evans, Excitation energy transfer in DNA: duplex melting and transfer from normal bases to 2-aminopurine Biochemistry 32 (1993) 12090–12095.

[11] S.S. Sastry, B.M. Ross, A direct real-time spectroscopic investigation of the mechanism of open complex formation by T7 RNA polymerase Biochemistry 35 (1996) 15715–15725.

[12] C.T. Martin, D.K. Muller, J.E. Coleman, Processivity in the early stages of transcription by T7 RNA polymerase Biochemistry 27 (1988) 3966–3974.

[13] J.R. Williamson, G-quartets in biology: reprise Proc. Natl. Acad. Sci. USA 90 (1993) 3124.

[14] J.R. Williamson, G-quartet structures in telomeric DNA Annu. Rev. Biophys. Biomol. Str. 23 (1994) 703–730.

[15] J. Grodberg, J.J. Dunn, *ompT* encodes the *Echerichia coli* outer membrane protease that cleaves T7 RNA polymerase during purification J. Bact. 170 (1988) 1245–1253.

[16] V. Zawadzki, H.J. Gross, Rapid and simple purification of T7 RNA polymerase Nucl. Acids Res. 19 (1991) 1948.

[17] K. Rajagopalan, A.J. Chavan, B.E. Haley, D.S. Watt, Synthesis and application of bidentate photoaffinity cross-linking reagents J. Biol. Chem. 268 (1993) 14230–14238.

[18] S. Sastry, B.M. Ross, RNA binding site in T7 RNA polymerase Proc. Natl. Acad. Sci. USA 95 (1998) 9111–9116.

[19] R.A. Velapoldi, K.D. Meinenz, A Fluorescence Standard Reference Material: Quinine Sulfate Dihydrate, National Bureu of Standards, Washington DC, 1980, pp. 260–264.

[20] M. Maslak, C.T. Martin, Effects of solution conditions on the steady-state kinetics of initiation of transcription by T7 RNA polymerase Biochemistry 33 (1994) 6918–6924.

[21] M.R. Eftink, in: J.R. Lakowicz (Ed.), Fluorescence Quenching, in Topics in Fluorescence Spectroscopy, 2, Principles, 1991, pp. 53–126.

[22] S.S. Sastry, J.E. Hearst, Studies on the interaction of T7 RNA polymerase with a DNA template containing a site-specifically placed Psoralen cross-link. I Characterization of elongation complexes J. Mol. Biol. 221 (1991) 1091–1110.

[23] R. Sousa, D. Patra, E.M. Lafer, Model for the mechanism of bacteriophage T7 RNAP transcription initiation and termination J. Mol. Biol. 224 (1992) 319–334.

[24] R. Guarjardo, R. Sousa, A model for the mechanism of polymerase translocation J. Mol. Biol. 265 (1997) 8–19.

[25] P.S. Song, K.J. Tapley, Jr., Photochemistry and photobiology of psoralens Photochem. Photobiol. 29 (1979) 1177–1197.
[26] P.-S. Song, Photoreactive states of furocoumarins Natl. Cancer Inst. Monogr. No. 66 (1984) 15–19.
[27] S.L. Driscoll, M.E. Hawkins, F.M. Balis, W. Pfleiderer, W.R. Laws, Fluorescenec properties of new guanosine analog incorporated into small oligonucleotides Biophys. J. 73 (1997) 3277–3286.
[28] J.F. Milligan, O.C. Uhlenbeck, Synthesis of small RNAs using T7 RNA polymerase Meth. Enzymol. 180 (1989) 51–62.
[29] W. Sundquist, S. Heaphy, Evidence for interstrand quadruplex formation in dimerization of human immunodeficiency virus I genomic RNA Proc. Natl. Acad. Sci. USA 90 (1993) 3393–3397.
[30] D. Sen, W. Gilbert, A sodium-potassium switch in the formation of four-stranded G4-DNA Nature (London) 344 (1991) 410–414.